Separation Science and Technology
Publication details, including instructions for authors and subscription information:
http://www.informaworld.com/smpp/title~content=t713708471

Computational Fluid Dynamics (CFD) Study of the Flow in an Annular Centrifugal Contactor

Kent E. Wardle[a]; Todd R. Allen[a]; Ross Swaney[b]
[a] Department of Engineering Physics, University of Wisconsin-Madison, Madison, WI, USA [b] Department of Chemical and Biological Engineering, University of Wisconsin-Madison, Madison, WI, USA

To cite this Article Wardle, Kent E. , Allen, Todd R. and Swaney, Ross(2006) 'Computational Fluid Dynamics (CFD) Study of the Flow in an Annular Centrifugal Contactor', Separation Science and Technology, 41: 10, 2225 — 2244
To link to this Article: DOI: 10.1080/01496390600745552
URL: http://dx.doi.org/10.1080/01496390600745552

Separation Science and Technology, 41: 2225–2244, 2006

ISSN 0149-6395 print/1520-5754 online
DOI: 10.1080/01496390600745552

Computational Fluid Dynamics (CFD) Study of the Flow in an Annular Centrifugal Contactor

Kent E. Wardle and Todd R. Allen
Department of Engineering Physics, University of Wisconsin–Madison, Madison, WI, USA

Ross Swaney
Department of Chemical and Biological Engineering, University of Wisconsin–Madison, Madison, WI, USA

Abstract: This study presents an initial scoping analysis of the application of computational fluid dynamics (CFD) to modeling the flow in an annular centrifugal contactor. The unsteady, turbulent nature of this multi-phase flow presents significant challenges to quantitative CFD modeling. Existing methods for confronting these obstacles are considered and initial results of the steady-state flow of a single liquid phase in the annular mixing zone are presented. The flow of particulates and the effects of changes in geometric and operational parameters were also evaluated. Even with simplifying assumptions qualitatively accurate results could be obtained using widely available CFD models.

Keywords: Solvent extraction, computational fluid dynamics, centrifugal contactors, reprocessing, liquid mixing

INTRODUCTION

The annular centrifugal contactor has been developed for use in solvent extraction processes used in the reprocessing of spent nuclear fuel. The compact size

Received 26 October 2005, Accepted 8 March 2006
Address correspondence to Kent E. Wardle, Department of Engineering Physics, University of Wisconsin–Madison, 1500 Engineering Drive, Madison, WI 53706, USA. E-mail: kwardle@wisc.edu

and efficiency of contactors have made them an attractive choice for a future fuel cycle facility which could be built to process existing light water reactor (LWR) fuel and advanced nuclear fuels. While a sufficient base of experience exists to facilitate successful operation of current contactor technology, a more complete understanding of the fluid flow within the contactor would enable further advancements in design and operation of future units. Computational fluid dynamics (CFD) may be a key tool which will provide both qualitative and quantitative analyses of the flow within the contactor and enable greater understanding of and confidence in scaled-up designs which would be used in pilot and full scale operational facilities.

The initial design of the annular centrifugal contactor was made at Argonne National Laboratory (ANL) by modification of a Savannah River Laboratory (SRL) contactor as described by Bernstein et al. (1) A cross-section for a generalized ANL contactor is shown in Fig. 1. Flows of immiscible liquids enter through ports into the annular or mixing region where the dispersion begins to form. Vanes below the rotor break the rotation of the dispersion and force the liquid into the rotor which then acts as a centrifuge separating the two phases and pumping the liquid up through the rotor. The separated phases then flow over the respective weirs and out the exit lines flowing by gravity to successive stages or collection vessels.

Extensive experimental work was performed throughout the 1980s by ANL researchers which expanded the ability to successfully design and operate contactors which could be used for a range of input compositions

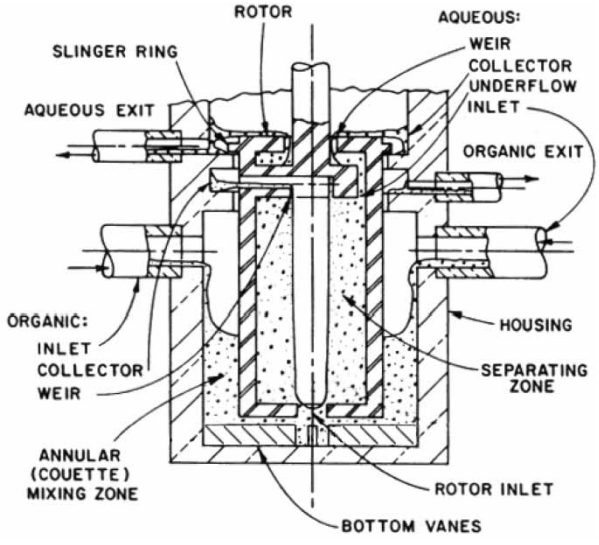

Figure 1. Sketch of the cross-section of an annular centrifugal contactor with the main components labeled. *Figure courtesy of Argonne National Laboratory.*

and flow rates. On the modeling front, the effort was primarily focused on descriptive correlation of experimental data; analytical methods were also implemented where possible. The dimensionless dispersion number was developed in order to predict the maximum throughput of a contactor for a given set of immiscible fluids and a fixed rotor speed (2). Significant effort was also put forth in the development of a computational model which could aid in the design of contactor weirs by calculating the necessary weir sizes given the properties of the two phases. A descriptive model for the height of the liquid in the annulus as a function of rotor speed was also developed. One area to which improved contactor modeling could contribute is the capability of predicting the liquid height in the annulus for a given set of conditions. Such knowledge is critical to optimized design and operation of the contactor. While the throughput of a given contactor is typically limited by the capacity for complete separation of the two phases within the rotor such that there is minimal other-phase contamination in the respective outlets, another limiting case is if the dispersion in the annulus fills the mixing zone and overflows into the organic collector ring. Even if the liquid height under nominal conditions is acceptable, flow transients and changes in liquid height due to phase inversion make the annular liquid height an important factor during operation.

For spent fuel processing operations the maximum contactor size is limited by uncertainty about the disposition of particulates in the contactor which results in size restrictions due to nuclear criticality concerns. Typically, feed streams are filtered to remove particulates remaining from incomplete dissolution of the spent fuel. It is also possible, however, for precipitates to form during processing. Application of CFD modeling to contactors would allow evaluation of the flow and formation of particulates.

This paper represents the initial phase of a modeling effort which attempts to provide an improved understanding of the flow within all regions of the contactor through the use of computational fluid dynamics including the prediction of annular liquid height, the flow of particulates and the flow in the separating zone. The initial phase of the study presented herein introduces some of the existing CFD tools which may provide insight into various aspects of the contactor problem. The initial results of the calculated steady-state, single-phase flow field in the mixing zone of a standard contactor geometry are presented as well as results for the residence time distribution of spherical particulates in the flow. The potential of CFD for evaluating contactor design and parameter changes is also demonstrated.

CFD Modeling of Contactors

While the applicability of computational fluid dynamics to a wide variety of problems has been greatly aided by the steady increase in computational

capability, there are still obstacles to rigorous treatment of a problem such as the centrifugal contactor. The flow in a centrifugal contactor is extremely turbulent, unsteady, and consists of at least three phases (two liquid phases and air). To accurately model the details of this kind of flow, each of these issues must be considered. A brief overview of these issues is given here as an introductory evaluation of the prospects for successful application of existing CFD methods to the contactor problem and it is anticipated that future research will focus on each of these issues individually and in greater detail.

While not specific to the contactor problem, the issue of turbulence always requires careful treatment. While more complicated techniques such as Large Eddy Simulation (LES) and full Reynold's Stress Models are available, Reynold's averaged Navier–Stoke's (RANS) solution methods such as the $k-\varepsilon$ method are still widely used for practical engineering problems as they have significantly less computational cost. Further, it has been shown that unsteady RANS solution methods are able to qualitatively and even quantitatively capture complex flows which are not statistically stationary (i.e. periodic vortex shedding) with much more accuracy compared to steady RANS solutions (3, 4).

There are also various methods for calculating the distribution of multiple phases within a computational domain (5–7). Some of the available methods are briefly described below.

VOF: The Volume of Fluid method was developed for tracking a liquid free surface such as a water/air interface. A single set of momentum equations is solved for the entire system and the volume fraction of each phase is tracked within each computational cell. In future studies this method will be applied to tracking the height of liquid in the annular (mixing) region.

ASM: The Algebraic Slip Mixture model tracks volume fraction of a dispersed phase in a continuous phase. As with the VOF method, a single set of momentum equations is solved for the entire system. The relative velocities of the dispersed and continuous phases are assigned via an algebraic slip velocity formulation. The dispersed phase droplet diameter must be specified and is typically assumed to be constant.

Eulerian: For this method, separate sets of momentum and continuity equations are solved for each of the phases in the system. Coupling of the phases is done through exchange coefficients. This method, although more complex than the ASM model, is probably the most applicable to modeling of the liquid–liquid dispersion formed in the contactor. It should also be possible to include the effects of interphase mass transfer using any of the above models.

Lagrangian: This method tracks individual particles or droplets as they move through the continuous fluid in a Lagrangian reference frame. These particles can interact with the continuous phase and exchange mass,

momentum, or energy. A key assumption of this method is that the dispersed phase occupies a small volume fraction. It is therefore not applicable to the liquid–liquid mixture as in the contactor system, but can be used to track the flow of particulates or calculate the residence time of a discrete fluid element within the contactor. Such calculations are performed within the context of this study.

While unsteady solution methods are well developed and relatively straightforward in their application, they greatly increase the computational burden of the problem. If a steady-state solution is desired, the system must be given some initial condition with the solution determined along finite time steps until steady state is assumed to have been achieved. At this point, the solution can be averaged over a given time period (number of time steps) to get a time-averaged, "steady-state" solution.

A problem comparable to the centrifugal contactor in terms of the computational modeling difficulties is the hydrocyclone separator, which separates particulates into different liquid streams using the centrifugal force of the swirling flow in the device. A good summary of the efforts which have been made to apply CFD to this issue is given by Nowakowski et al. (8) As with the contactor, this piece of equipment also involves turbulent swirling flow of multiple phases and therefore provides a good comparison for validation of computational techniques. The Lagrangian method of particle tracking mentioned above has been applied to the prediction of particle distribution and the simulation results were in agreement with experimental values (9). Interestingly, during operation of the hydrocyclone an "air core" develops in the center of the spinning fluid (10). Along the axis of the rotor within the separation zone of a contactor there is also a core of rotating air which may add some complexity to the modeling of this region. Olsen and Van Ommen (11) report successful modeling of this air core using the ASM multi-phase model. They reported the use of CFD modeling to hydrocyclone design optimization and have found good agreement with experimental results.

MODELING METHODS

Contactor Geometry and Mesh

While the mixing zone nominally extends along the entire length of the annular region from the base of the contactor housing to the fluid inlets (see Fig. 1), in order to minimize the volume of the computational domain, the mixing zone was only modeled to a height of 3 cm above the rotor bottom ($\sim$3 cm below the inlets). The modeled contactor geometry is given in Fig. 2 and the significant geometric parameters are listed in Table 1. The radius ratio (ratio of rotor radius to housing radius) is also listed rather than

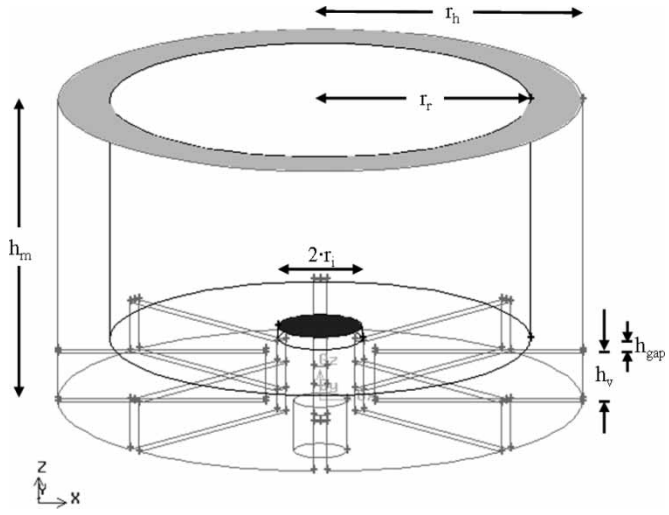

Figure 2. Model geometry with the major parameters labeled and showing the annular inlet (located at $z = h_m$, light grey) and outlet (dark grey) as shaded surfaces.

the absolute width of the annular gap, as it is an important parameter for scale up of contactors. The model geometry was based on a commercially available CINC-V2 contactor unit. The computational volume was assumed to be completely full of a single liquid phase, water, and the inlet to the annular region was assumed to be flat and perpendicular to the rotor surface for simplicity. In reality, for typical inlet water flow rates in the same size contactor at similar rotor speeds (3000 RPM), the liquid height in the mixing zone ranges from 1.5 to 2.0 cm above the rotor edge and the free surface does not appear to be flat. Despite these departures, the solution for these approximated conditions will provide a starting point for understanding the flow in the mixing zone and should provide a physically realistic solution for the flow underneath the rotor. Two-phase air/water calculations which attempt to model the free

Table 1. Key geometric parameters of model

Parameter	Symbol	Value
Rotor radius	r_r	2.54 cm
Housing radius	r_h	3.17 cm
Radius ratio	r_r/r_h	0.801
Rotor inlet radius	r_i	0.505 cm
Vane height	h_v	0.617 cm
Vane-to-rotor gap	h_{gap}	0.159 cm
Mixing zone height	h_m	3.776 cm

surface and include the full length of the mixing zone will be included in future efforts.

A grid resolution study was conducted to determine the dependence of the solution on the grid spacing. The mesh was refined primarily near the rotor as this is a high shear region with the largest velocity gradients. Along with properties such as the rotor shear stress, volume-average tangential velocity, and axial fluid velocity at the midpoint of the rotor inlet, the parameter y^+ at the rotor wall was also monitored for successively finer meshes. The parameter y^+ (equation (1)) is a dimensionless measure of the near-wall mesh and is a function of the fluid density ρ and viscosity μ, the friction velocity u_τ, and the distance from the wall y.

$$y^+ = \frac{\rho u_\tau y}{\mu} \tag{1}$$

The friction velocity u_τ is determined from the shear stress at the wall τ_w by

$$u_\tau = \left(\frac{\tau_w}{\rho}\right)^{1/2} \tag{2}$$

Standard wall functions, as were used in this study, are valid for $y^+ > 30$ and therefore it was desired that the final mesh have a value of $y^+ \approx 30$. The final meshing scheme that was used for all the geometries in this study employed a quadrilateral mesh on the rotor side with spacing of 0.04 cm and 0.125 cm tetrahedral meshing for the rest of the volume as shown in Fig. 3(a). In this way, the fine mesh of the base geometry consisted of 588484 tetrahedral cells. All meshes were generated using Gambit 2.1.6. from Fluent Inc.

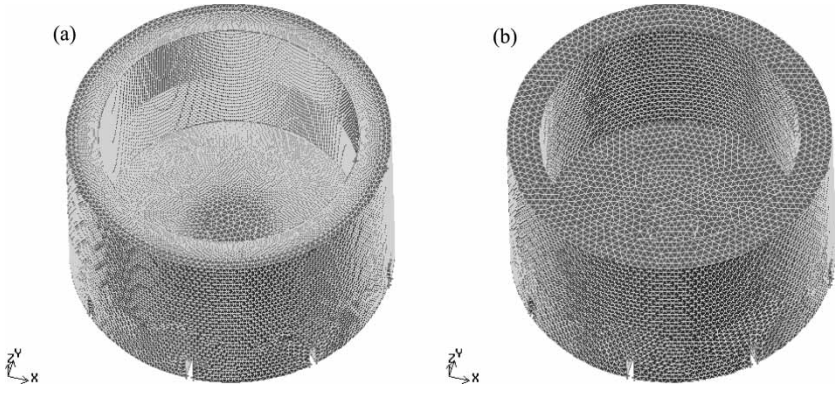

Figure 3. Contactor model mesh for FLUENT calculations. (a) Fine mesh consisting of a 0.04 cm quadrilateral mesh on the rotor surface and 0.125 cm tetrahedral mesh elsewhere used for all final solutions. (b) Coarse tetrahedral mesh with 0.15 cm spacing used for initial calculations.

Modeling Conditions and General Solution Method

Calculations of the steady-state flow solution were done using the commercially available FLUENT 6.1 which uses a finite volume solution method. For all calculations, turbulence was modeled using the RNG $k-\varepsilon$ turbulence model and standard wall functions. FLUENT's default under-relaxation factors, interpolation schemes, and pressure-velocity coupling were used. The inlet was defined by a constant mass flowrate of 0.01 kg/s ($\sim$600 mL/min) of water and the outlet was specified as a constant pressure boundary. The rotor and housing walls both had no-slip conditions and the rotor wall was also given a fixed rotational velocity. A rotor speed of 3000 RPM was assigned as the base case, but solutions for 1000 and 2000 RPM are also presented to evaluate changes in the flow due to rotor speed.

The solution method applied to the various cases was the same. A coarse mesh, consisting of a uniform tetrahedral grid with a spacing of 0.15 cm (Fig. 3(b)), was generated and the solution for this coarse mesh was first calculated. Due to the high shear at the rotor wall boundaries it was necessary to also incrementally increase the rotor rotation rate up to the desired value in order to achieve a converged final solution. Typically, the coarse solution was initially calculated for 1000 RPM and the rotation rate was increased in increments of 1000 RPM. The solution was not taken completely to convergence at the intermediate steps except where results are presented. With a converged solution for the desired rotor speed on the coarse mesh, it was then possible to interpolate this solution onto the final, fine mesh and calculate the solution. In this way, no changes in rotor speed were necessary on the final mesh, minimizing computational time.

RESULTS AND DISCUSSION

General Flow

The base case geometry was taken to be the geometry given in Fig. 2 and Table 1 with a rotor speed of 3000 RPM. In general, the flow patterns observed in the CFD model were found to be comparable to those seen during actual contactor operation (with a transparent housing). Velocity vectors on a horizontal (Fig. 4) and vertical plane (Fig. 5) for the solution of the base case show the direction and relative magnitude of the flow field. It is apparent from Fig. 4 that there are swirling patterns within the area between each of the vanes beneath the rotor. From Fig. 5 it is clear that as would be expected, the flow of the highest magnitude is located near the rotor with a maximum value approximately at the axial center of the rotor. This behavior can be seen more clearly in Figs. 6 and 7 which show the radial and axial flow components, respectively.

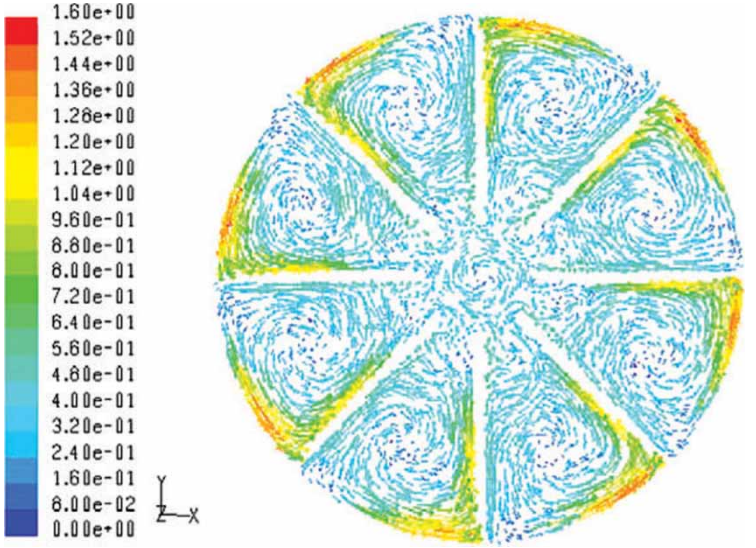

Figure 4. Velocity vectors on horizontal plane midway between housing bottom and rotor bottom colored by velocity magnitude (m/s).

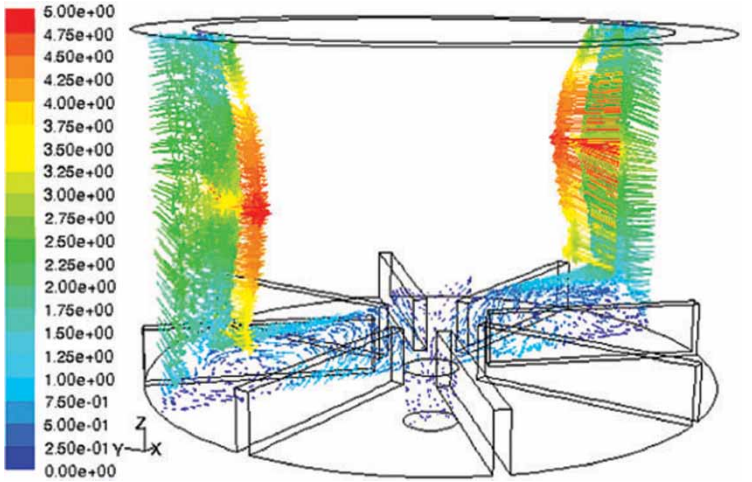

Figure 5. Velocity vectors colored by velocity magnitude (m/s) on a vertical cross-sectional plane which bisects the region between vanes. The plane is shown at an angle to emphasize the direction and relative magnitude of vectors near rotor.

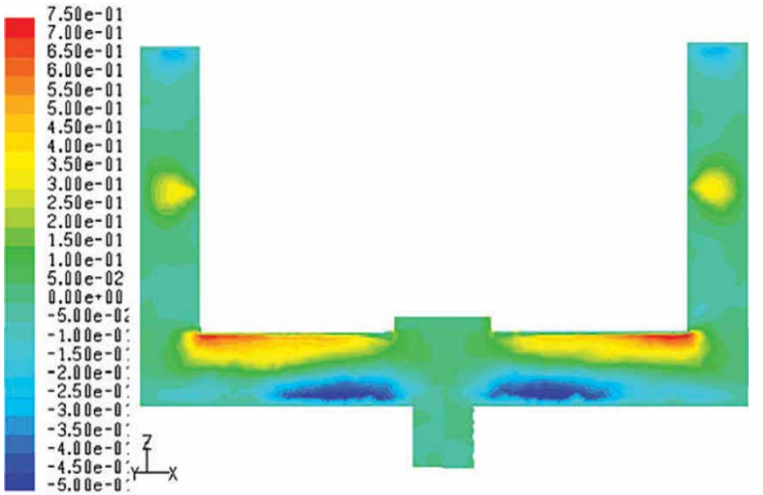

Figure 6. Radial velocity contours (m/s) on a vertical cross-section of the contactor mixing zone (see Fig. 5 for the relative orientation of the plane). Positive radial velocity is defined as flow out from the rotor axis.

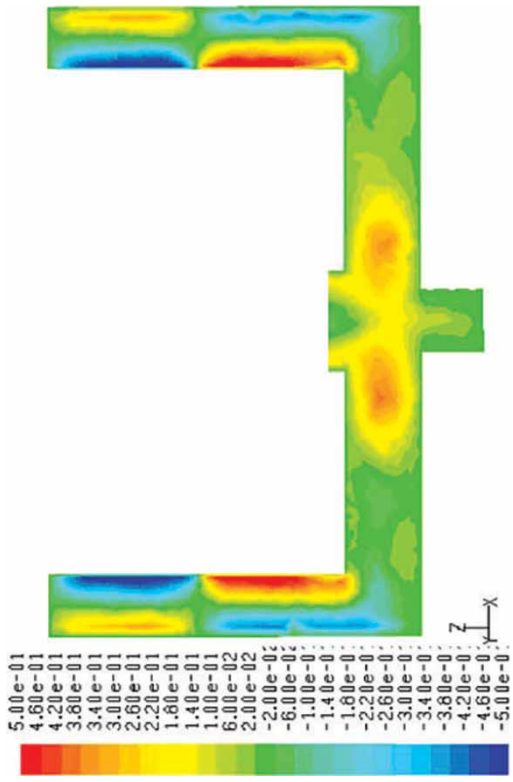

Figure 7. Contours of axial velocity (m/s) in which positive axial velocity is defined as flow upward or in the positive z-direction. Refer to Fig. 5 for the relative orientation of the plane.

From Fig. 6 a separation point from the side of the rotor is evidenced by the region of positive radial velocity (yellow). Figure 7 shows that the fluid region above this point is moving downward near the rotor and upward near the housing wall while the region below this point is flowing in the opposite direction—upward near the rotor and down at the housing wall. This flow pattern is characteristic of Taylor Couette flow. While the stability of these "Taylor vortices" cannot be shown without a transient solution, by experimental observation they are very unstable and oscillatory. Transient CFD simulations might enable the analysis of the oscillations as a method of comparison between changes in geometric and operational parameters.

Particle Tracking

Tracking particles released from a specified point can provide useful information regarding the disposition of particulates (or droplets) in the volume. Particle tracking was performed using FLUENT's Discrete Phase Model (DPM) which applies a Lagrangian approach to tracking particles of specified diameter and density through the system. Particle trajectories are solved by stepwise integration in time over a specified number of path length increments. For this method, it was assumed that the particles were in such small quantities that they do not affect the flow of the continuous phase. Two thousand particles of a specified density and diameter were injected with a zero initial velocity at a radial point in the center of the annulus on the inlet surface. Particles were tracked sufficiently long such that greater than 95% of the particles exited the system. Turbulence was accounted for stochastically by allowing for random fluctuation of the instantaneous velocity proportional to the local turbulence intensity for each point along the integration path. Residence time was defined as the total flow time from the point of release until the particle exited the volume through the outlet.

It was observed that as the particle diameter (and consequently its mass) was increased, the average particle residence time increased (see Fig. 8). For $10\,g/cm^3$ particles, such as would be found due to poorly dissolved fuel ($\rho_{UO_2} \approx 10\,g/cm^3$), the longer residence time was a result of particles not being able to pass through the first Taylor vortex. Particles are spun out from the rotor to the outer wall where the fluid is actually rising and therefore they are less likely to get below the height of the separation point on the rotor side. The particles appear to spend most of the time in this upper vortex, but once they get below the separation line into the lower region they typically quickly pass out of the volume (into the rotor). Particles larger than a critical diameter of $\sim$20 microns rarely if at all were able to pass below the separation line and became trapped in the upper vortex. As the particle diameter was increased further, the particles tended to stay progressively closer to the top of the annular region. These results were for relatively dense particles and it would seem that for lighter

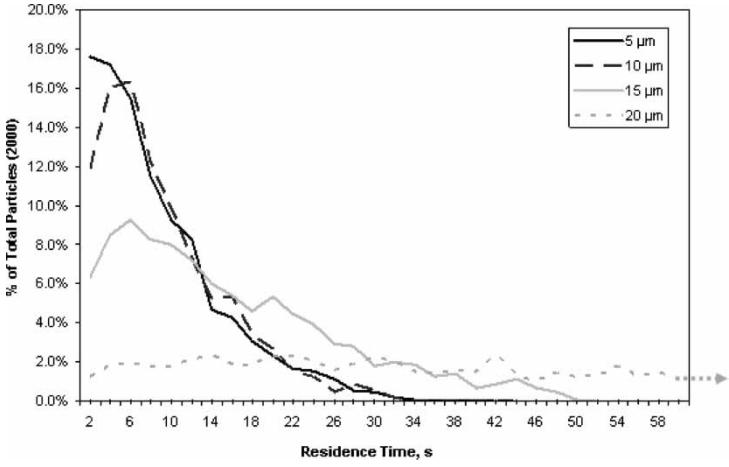

Figure 8. Particle residence time distribution for four different particle diameters ($\rho = 10\,\mathrm{g/cm^3}$). The distribution for the largest diameter particle ($\mathrm{d} = 20\,\mu\mathrm{m}$) is approximately constant through $\sim$180 s.

particles (still more dense than water), such as would be representative of insoluble nitrate salts, the critical particle size would be larger.

As for particles less dense than water ($\rho = 0.8\,\mathrm{g/cm^3}$), there were no general obstacles to flow through the volume except for very large particles ($\mathrm{d} > 0.2$–0.25 mm) which, in contrast to dense particles, appeared to migrate toward the region near the separation line at the side of the rotor. It is possible to consider particles of this density as organic fluid particles such as kerosene, however, it has been shown that for liquid–liquid dispersions under the given conditions the droplet diameter would be an order of magnitude smaller than these values (12).

Another important class of particles are those which are neutrally buoyant such as might be representative of Pu(IV) colloidal polymers which have been found to form in PUREX processes (13, 14). The trajectories of $1\,\mathrm{g/cm^3}$ particles of various diameters were calculated using the same methods, but in general these particles did not exhibit any notable behavior (i.e. change in residence time) in the mixing zone. It should be noted, however, that the assumption of spherical particles as used in these calculations is likely not true of Pu(IV) colloidal particulates which in general are known to have an elongated, cylindrical shape (13).

While in each of these cases the density was held constant and the diameter was increased thus increasing particle mass, it would be possible to repeat the calculations for constant mass particles of increasing diameter or constant diameter particles of increasing mass in order to individually analyze the effects of drag (particle diameter) and momentum (particle mass).

Parameter Changes

Rotor Speed

The effect of the rotor speed was evaluated by comparing the converged solutions for rotor speeds of 3000 (base case), 2000, and 1000 RPM. In general, the flow field was similar with only relative changes in magnitude. This would be expected for the present system as the volume was assumed fully liquid; however, during actual operation of contactors changes in rotor speed result in changes in the annular liquid level. Figures 9 and 10 show the axial velocity along a horizontal line beneath the rotor and the radial velocity along a vertical line running along the center of the annulus. From Fig. 9 it is clear that beneath the rotor, a decrease in rotor speed only decreases the relative magnitude of the flow field without significantly affecting the radial location of the maxima and minima. In the annular region (Fig. 10), the axial height of the separation point on the side of the rotor decreases with decreasing rotor speed.

Geometry

The number of vanes beneath the rotor was decreased from eight as in the base case to only four in order to observe changes in the calculated flow field as a result of a change in a geometric parameter. The grid generation and solution methods were the same as for the other cases.

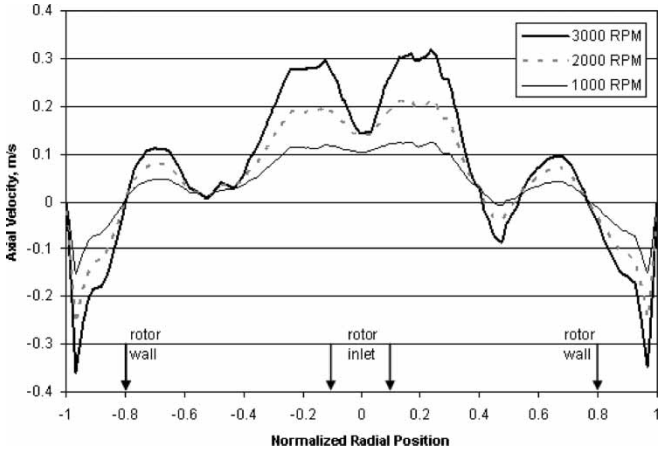

Figure 9. Axial velocity (m/s) as a function of radial position (normalized by the housing radius) along a horizontal line midway between the bottom of the housing and the rotor bottom for rotor speeds of 3000 (base), 2000, and 1000 RPM.

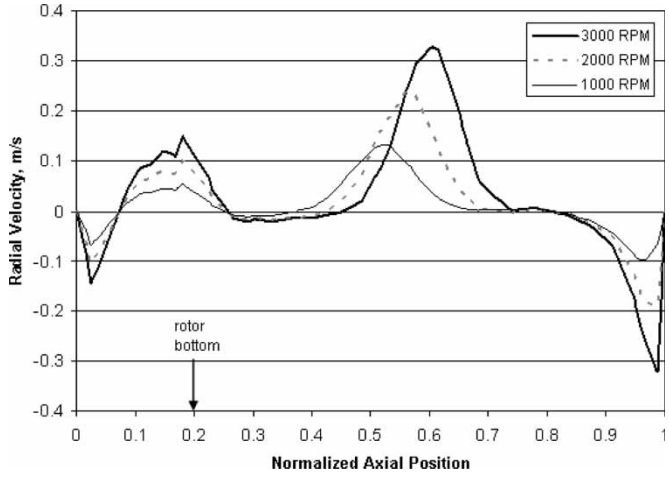

Figure 10. Radial velocity (m/s) as a function of axial position (normalized by the mixing zone height) along a vertical line midway between the rotor and housing for the three rotor speeds.

As might be expected, there was little difference in the flow in the annulus for the geometry change beneath the rotor. As for flow under the rotor, Fig. 11 shows the areas of rotation that were evident in the base geometry (see Fig 5) have been shifted toward the rotor axis resulting in a more significant area of swirl centered on the rotor axis. The result of this swirling region around the rotor axis is a decrease in the magnitude of positive axial flow near the rotor axis as shown in Fig. 12. This plot also shows that the regions of positive axial flow that were near the outer edge of the rotor ($r \approx \pm 0.8$) for the base geometry have been pushed radially outward.

CONCLUSIONS

This study has presented the results of CFD calculations of the flow in the mixing region of an annular centrifugal contactor applying various simplifying assumptions (i.e. steady-state, liquid full contactor, and single liquid phase) and using relatively simple CFD models. It was found that realistic, qualitatively accurate results could be obtained for the flow underneath the rotor. In the annular region above the rotor bottom, the accuracy of the solution is dependent upon the validity of the assumptions that the entire region is full of liquid and that gradients on the inlet surface are negligible. Under typical conditions the actual flow in the annulus is largely a free surface flow and it is not clear whether contact between the fluid and the rotor is continuous or intermittent. Therefore, to look at the

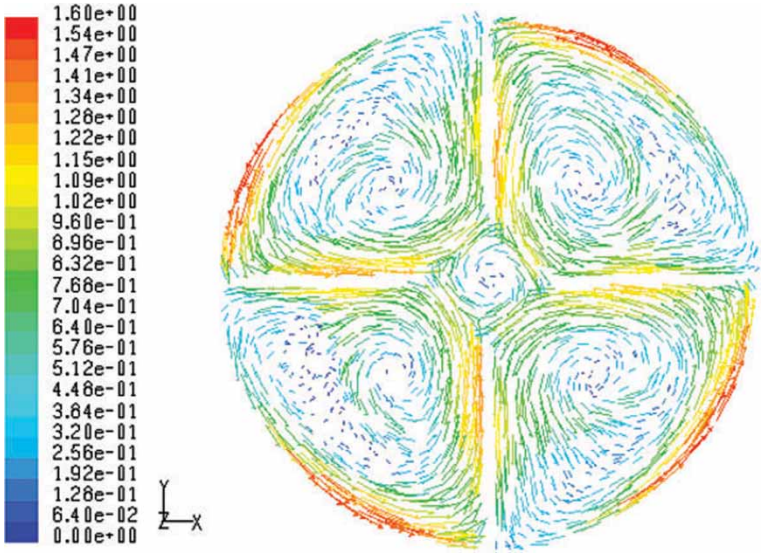

Figure 11. Vectors of velocity magnitude (m/s) on a horizontal plane midway between the rotor bottom and housing bottom.

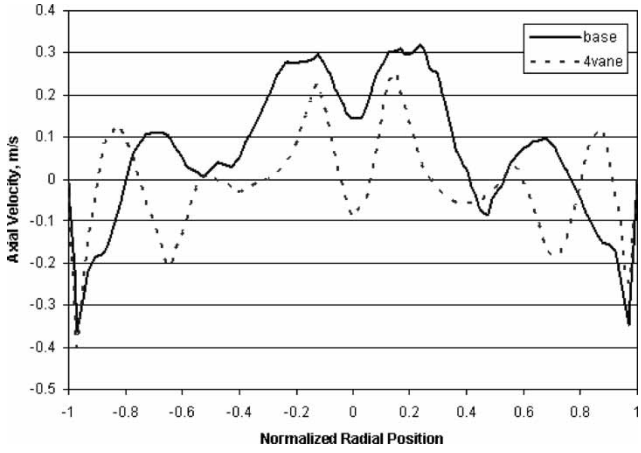

Figure 12. Comparison of axial velocity (m/s) profiles along a horizontal line beneath the rotor bisecting the region between vanes for both the base geometry (eight vanes) and the modified four vane geometry.

actual characteristics of flow in the annular region of the mixing zone in a quantitative manner transient, two-phase calculations will need to be performed.

Regarding the flow of particulates, the calculations performed in this study provide a starting point for understanding the factors which may limit particle transport within the mixing zone. The method of calculating particle tracks from the flow solution was successfully applied. As future modeling efforts include more aspects of the flow (i.e. multi-phase and transient) and model flow in both the mixing and separation zones this method should yield very useful results regarding the disposition of particulates in the entire contactor system and the contact times of different phase fluid elements.

It was also demonstrated that CFD could be useful in evaluating the effect of contactor design and operational changes. However, analysis of the extent of dispersion formation and mixing between the organic and aqueous phases may be essential to providing a quantitative comparison needed to evaluate design modifications and will require solutions including both phases. Future efforts will also need to include modeling of the separation zone inside the rotor which may introduce unique difficulties regarding boundary conditions and convergence.

Further effort to apply CFD methods to the analyzing the flow in the annular centrifugal contactor is warranted. More detailed calculations should help to understand the quantitative accuracy possible. Above all, the results from more quantitative calculations will need to be validated against experimental results and observations. However, without a significant experimental effort in tandem with this computational effort, such comparison

would have to focus mainly on easily measurable quantities (such as the annular liquid height) as very limited contactor data are available. At present there have been no quantitative measurements of the flow field in the contactor with which to validate the simulations. While the flow in the annulus has been observed directly by use of a transparent contactor housing, a similar understanding of the flow in the separation zone (i.e. shape of liquid–liquid interface) has not been obtained. In general, more detailed experimental information will be required as more detailed simulation methods are applied.

ACKNOWLEDGEMENTS

The authors would like to acknowledge Argonne National Laboratory for technical support of this research effort. In particular, Kent Wardle would like to thank Candido Pereira of the Chemical Engineering Division and Roald Wigeland of the Nuclear Engineering Division for helpful conversations. This research was performed under appointment to the U.S. Department of Energy Nuclear Engineering and Health Physics Fellowship Program sponsored by the U.S. Department of Energy's Office of Nuclear Energy, Science, and Technology.

REFERENCES

1. Bernstein, G., Grosvenor, D., Lenc, J., and Levitz, N. (1973) A high-capacity annular centrifugal contactor. *Nucl. Technol.*, 20: 200.
2. Leonard, R., Bernstein, G., Pelto, R., and Ziegler, A. (1981) Liquid–liquid dispersion in turbulent Couette flow. *AICHE J.*, 27: 495.
3. Wegner, B., Maltsev, A., Schneider, C., Sadiki, A., Dreizler, A., and Janicka, J. (2004) Assessment of unsteady RANS in predicting flow instability based on LES and experiments. *Int. J. Heat and Fluid Flow.*, 25: 528.
4. Iaccarino, G., Ooi, A., Durbin, P., and Behnia, M. (2003) Reynold's averaged simulation of unsteady separated flow. *Int. J. Heat and Fluid Flow.*, 24: 147.
5. Calay, R. and Holdo, A.. CFD modelling of multiphase flows–an overview, in *Pressure Vessels and Piping 2003*, Vol 460, ASME, 83.
6. Lun, I., Calay, R., and Holdo, A. (1996) Modelling two-phase flows using CFD. *Applied Energy*, 53: 299.
7. Fluent Inc. *Fluent 6.1 User's Guide*, 2003.
8. Nowakoski, A., Cullivan, J., Williams, R., and Dyakowski, T. (2004) Application of CFD to modelling of the flow in hydrocyclones. Is this a realizable option or still a research challenge? *Minerals Eng.*, 17: 661.
9. Narasimha, M., Sripriya, R., and Banerjee, P. (2005) CFD modelling of hydrocyclone—prediction of cut size. *Int. J. Miner. Process.*, 75: 53.
10. Cullivan, J., Williams, R., Dyakowski, T., and Cross, C. (2004) New understanding of a hydrocyclone flow field and separation mechanism from computational fluid dynamics. *Minerals Eng.*, 17: 651.

11. Olsen, T.J. and Ommen, R.V. (2004) Optimizing hydrocyclone design using advanced CFD model. *Minerals Eng.*, 17: 713.
12. Zhu, X. and Vigil, D. (2001) Banded liquid–liquid Taylor-Couette-Poiseuille. *AICHE J*, 47: 1932.
13. Thiyagarajan, P., Diamond, H., Soderholm, L., Horwitz, E.P., Toth, L., and Felker, L. (1990) Plutonium(IV) polymers in aqueous and organic media. *Inorg. Chem.*, 29: 1902.
14. Scoazec, H., Pasquiou, J., and Germain, M. (1990) Some plutonium IV properties in PUREX process. *I. Chem. E. Symposium Series*, 119: 221.